Curvature-driven growth and interfacial noise in the voter model with self-induced zealots

Luís Carlos F. Latoski [1,*] W. G. Dantas [2,†] and Jeferson J. Arenzon [1,3,‡]
[1] Instituto de Física, Universidade Federal do Rio Grande do Sul, CEP 91501-970, Porto Alegre, Rio Grande do Sul, Brazil
[2] Departamento de Ciências Exatas, EEIMVR, Universidade Federal Fluminense, CEP 27255-125, Volta Redonda, Rio de Janeiro, Brazil
[3] Instituto Nacional de Ciência e Tecnologia–Sistemas Complexos, Rio de Janeiro, 22290-180, Rio de Janeiro, Brazil

(Received 7 April 2022; accepted 27 June 2022; published 18 July 2022)

We introduce a variant of the voter model in which agents may have different degrees of confidence in their opinions. Those with low confidence are normal voters whose state can change upon a single contact with a different neighboring opinion. However, confidence increases with opinion reinforcement, and above a certain threshold, these agents become zealots, irreducible agents who do not change their opinion. We show that both strategies, normal voters and zealots, may coexist (in the thermodynamical limit), leading to competition between two different kinetic mechanisms: curvature-driven growth and interfacial noise. The kinetically constrained zealots are formed well inside the clusters, away from the different opinions at the surfaces that help limit their confidence. Normal voters concentrate in a region around the interfaces, and their number, which is related to the distance between the surface and the zealotry bulk, depends on the rate at which the confidence changes. Despite this interface being rough and fragmented, typical of the voter model, the presence of zealots in the bulk of these domains induces a curvature-driven dynamics, similar to the low temperature coarsening behavior of the nonconserved Ising model after a temperature quench.

DOI: 10.1103/PhysRevE.106.014121

I. INTRODUCTION

Consensus, in physical models of opinion dynamics [1–3], may be achieved locally, within a given subgroup, or globally, with all interacting agents agreeing on a common position. Understanding the process of the formation and the probability of attaining consensus, how to enforce it, and why it is sometimes prevented is important to uncover its underlying, universal mechanisms. An example is the convergence of results in some scientific fields (vaccines, climate, etc.) that, despite being widely accepted in the scientific community [4,5], do not always lead to evidence-based public policies. Indeed, in actual situations, agreement with other individuals may depend on several factors (e.g., the local network, the intensity of noise, new evidence, propaganda, fake news, self-confidence, and other psychological reinforcement mechanisms). However, in simple systems like the binary voter model (VM) and related models of language competition, the process is simplified and considered an ordering one, in which each agent aligns its opinion with one of its neighbors. In an infinite, regular lattice of dimension $d \leqslant 2$, the consensus in the VM is an absorbing state (bulk noise is absent) and is always attained, albeit with very different time dependences [6–9]. In two dimensions, the geometry we consider here, the growth of order by coarsening, in the absence of surface tension, is not driven by the curvature of the interfaces but by its noise [10,11].

In the original VM, agents have no confidence whatsoever, and opinions may change upon a single contact with a different position. The possibility of having strong confidence is among the many modifications introduced to better describe more complex social phenomena [1–3]. These confident agents, or zealots, may never change their opinion or may change it in spite of the opinions of their neighbors [12–16], introducing some disorder in the system that, besides interfering with how local consensus groups grow, may even prevent the system from attaining global consensus. When intermediate levels of confidence are allowed, the zealot state may be transient [17–26], and opinions are kept while the necessary number of contacts is not attained (complex contagion). This is akin to annealed disorder and represents the inertia in the process of changing an opinion, associated with a reinforcement mechanism that makes positions stronger or weaker. The necessity of multiple contacts prior to a change in state is similar to sampling the local field by interacting with a larger number of closest neighbors [17]. This noise reduction mechanism induces an effective surface tension [17,20,22,26–32], and some properties become analogous to those of the low temperature coarsening of the Ising model with nonconserved order parameters in the Allen-Cahn (model A) universality class [33] (hereafter IM0).

We propose an alternative model in which, instead of zealotry being an inherited characteristic, it may develop depending on the previous history of an individual. While its confidence is low, the agent behaves as a normal voter. However, above a given threshold its opinion freezes, and it becomes a kinetically constrained zealot. This self-induced disorder may be either irreversible (quenched) or, when the confidence keeps evolving, reversible (annealed). A

*luis.latoski@ufrgs.br
†wgdantas@id.uff.br
‡arenzon@if.ufrgs.br

 ©2022 American Physical Society

reversible, or transient, zealot needs multiple interactions with the opposite opinion in order to reset its confidence and once again be able to change its opinion. This resetting corresponds to a complex contagion process, different from the simple, single contact process for normal agents. During the dynamics, clusters of agents with a common opinion form, grow, and compete for the consensus state. The reinforcement process between agents with the same opinion leads, after multiple interactions, to the formation of zealots in the bulk of these clusters. Because of the constant flipping that occurs close to the surface where both opinions coexist, the confidences are repeatedly reset, the agents tend to be normal voters, and consequently, the surface is very rough and fragmented. Below the actual interface there is another one that is internal, separating the bulk zealots from normal voters, all with the same opinion. Close to this secondary surface, normal voters who are close to zealots have a persistent neighborhood that induces an increase in their confidence, eventually increasing the probability of the normal voters becoming zealots themselves. This seems to be the mechanism responsible for the effective surface tension of the internal surface, which behaves as a frame structure for the external one. An important question is whether the internal surface is enough to turn the dynamics into a curvature-driven one, in spite of the interface still being rough as in the original VM. Moreover, what are the consequences for the probability of attaining a consensus? How does the approach to the stationary state change, depending on the parameters of the model? How do the geometric properties of the opinion clusters (neighboring agents with the same opinion) differ from those of the pure VM? These are some of the questions that we try to answer in the following sections.

II. THE MODEL

The state of each agent is characterized by two variables, (σ_i, η_i). The binary opinion is represented by the discrete variable $\sigma_i = \pm 1$, where $i = 1, \ldots, N$. The total number of agents N corresponds to the sites either in a one-dimensional (1D) ring or in a two-dimensional (2D) square lattice where $N = L^2$. Each opinion is associated with some individual degree of confidence, which is described by the continuous variable $\eta_i \geqslant 0$. It depends on the previous history of contacts and evolves after each interaction. When η_i attains the threshold ϕ (which is set to $\phi = 1$), the agent becomes refractory to the opinions of its neighbors, and σ_i is temporarily frozen, a form of self-induced disorder. However, η_i keeps evolving, and when it get smaller than ϕ, that agent becomes, once again, susceptible to the opposite opinions of its nearest neighbors, and σ_i may change. We will refer to transient zealots simply as "zealots," while the other agents will be called "normal."

In a Monte Carlo step (MCS), N attempts to update randomly chosen agents are performed. Two agents are selected, i and one of its nearest neighbors, j, whose states are, respectively, (σ_i, η_i) and (σ_j, η_j) at time t. If their opinions differ, $\sigma_i \neq \sigma_j$, and $\eta_i < \phi$, the nonzealot focal site changes its opinion and aligns with j:

$$\sigma_i \longrightarrow \sigma_j \quad \text{if } \eta_i < \phi. \tag{1}$$

Although zealots, obviously, do not change their opinions, the confidences of both i and j are updated, in this case, accordingly, with

$$\eta_i \longrightarrow \eta_i/\gamma, \tag{2}$$

$$\eta_j \longrightarrow \eta_j + \Delta\eta, \tag{3}$$

where γ and $\Delta\eta$ are positive parameters. The fact that i is confronted with a different opinion is enough to change its confidence by the rescaling factor γ. For intermediate values, $1 < \gamma < \infty$, η_i continuously decreases, and zealots eventually may become normal once again. When $\gamma \leqslant 1$, η_i does not decrease, and becoming a zealot is an irreversible process that may prevent the system from attaining a consensus. This mimics the reinforcement observed among conspiracy theorists and among negationists. The confidence of the neighbor j, on the other hand, always increases by $\Delta\eta$ because j had the opportunity to express its opinion to a neighbor. Finally, when both agents have the same opinion, $\sigma_i = \sigma_j$, the mutual reinforcement is positive, and both confidences increase:

$$\eta_{i,j} \longrightarrow \eta_{i,j} + \Delta\eta. \tag{4}$$

We study the above competing mechanisms in the extreme cases $\gamma = 1$ and $\gamma \to \infty$. If $\gamma \to \infty$ and $\sigma_i \neq \sigma_j$, the confidence of the focal agent is always reset; that is, η_i instantly becomes zero. Thus, whatever the degree of zealotry, only two steps may be enough for any agent to change its opinion: in the first interaction the confidence is reset, and in the next step the opinion may be updated. In this way, the model combines simple and complex contagion, in which single or multiple exposures are necessary, respectively, to induce a change in opinion. The other case, $\gamma = 1$, corresponds to the irreversible limit where the confidence never decreases and the system becomes frozen once all η_i become larger than ϕ. Irrespective of the value of γ, in the initial steps of the dynamics, when zealots have not yet been created, the model is equivalent to the standard VM, but there is a γ-dependent timescale when it crosses over to a new behavior. The main objective of this paper is, indeed, to describe and understand how the behavior is affected by the presence of irreducible agents.

III. RESULTS

A. One dimension

Initially, the variables $\{\sigma_i\}$ characterizing the opinion of all N sites are randomly assigned, chosen with equal probability of being $\sigma_i = \pm 1$. The initial level of confidence, instead, is the same for all agents, $\eta_i = 0$. Although we have performed simulations with several different sizes of the 1D ring, we present only the results for $N = 10^5$, which is enough to reduce finite size effects. All results are averaged over 100 samples. An important observable is the fraction of links connecting neighboring agents with different opinions (defects) $\rho(t)$. In addition to it, we also consider the persistence $P(t)$, the fraction of sites that have not changed their initial state up to time t [34].

Figure 1 shows the temporal evolution of both $P(t)$ and $\rho(t)$. Since zealots appear only later in the dynamics (solid red line), the initial trend is the same as the VM: $P(t) \sim t^{-3/8}$ [35,36] and $\rho(t) \sim t^{-1/2}$ [8]. However, along with the

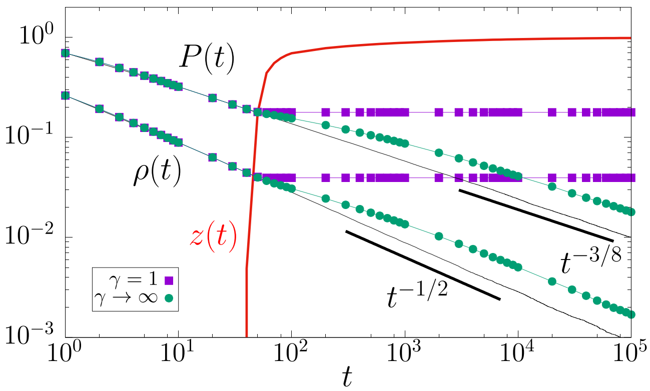

FIG. 1. Persistence $P(t)$ and density of defects $\rho(t)$ in one dimension for $\Delta\eta = 10^{-2}$ and $\gamma = 1$ (purple symbols) and $\gamma \to \infty$ (green symbols). The solid black curves correspond to the pure 1D VM where $P(t) \sim t^{-3/8}$ [35,36] and $\rho(t) \sim t^{-1/2}$. The red curve shows the very fast increase in the fraction of zealots $z(t)$. There are three different regimes. In the initial one, the system follows the VM behavior. It is followed by an intermediate regime that starts when zealots first appear, and the curves deviate from the VM behavior. Eventually, in the third regime, the system returns to the exponents characterizing the VM behavior.

fast increase in the density of zealots, we observe deviations from the VM behavior. For $\gamma = 1$, once zealots are created, the system ends in a frozen configuration with two or more compact blocks of opposite opinions, and consensus is never achieved. On the other hand, for $\gamma \to \infty$, both $P(t)$ and $\rho(t)$ slow their decrease in a transient interval, soon returning to the VM exponent at longer times, albeit with a larger coefficient.

The different temporal regimes are illustrated in the snapshots in Fig. 2. In the initial regime in the left panel, zealots are absent, and the dynamics is the same as the VM. The system is divided into small domains that coalesce once two walls collide [37]. In the intermediate regime in the middle panel, zealots appear (dark colors) in the interiors of the domains. Normal agents with both opinions (light colors) become con-

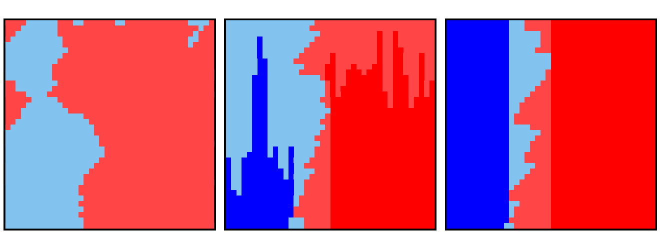

FIG. 2. Snapshots for the 1D case with $\gamma \to \infty$ and $\Delta\eta = 10^{-2}$, showing the temporal evolution in the three different regimes (time goes from top to bottom, and only part of the lattice is shown). Dark colors are used for zealots, while normal voters ($\eta_i < \phi$) are indicated by light colors. In the initial regime (left panel), the dynamics is indistinguishable from the original VM, and several small domains coexist. The middle panel shows the intermediate regime, where many of these domains have already coalesced and the first zealots appear away from the interfaces. Finally, the right panel illustrates the long time behavior, where there are two compact blocks of zealots with opposite opinions and, in the middle, a region with normal agents.

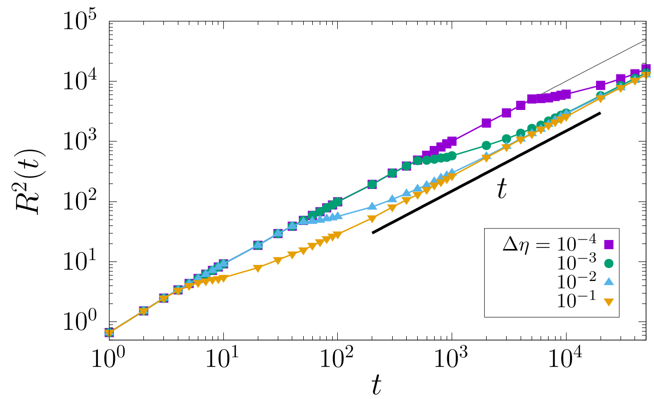

FIG. 3. Mean square displacement $R^2(t)$ of the single wall for different values of $\Delta\eta$. The thin black line is the linear, diffusive behavior of the VM. At both short and long times, the behavior is diffusive, $R^2(t) \sim t$, for all values of $\Delta\eta$. There is, however, an intermediate, subdiffusive regime in which the curves depart from and, later, return to the linear behavior.

fined between compact blocks of zealots, characterizing the late stage of the dynamics in the right panel. Inside these stripes, the normal agents follow the VM, and once the moving border (where light red and light blue are neighbors) gets closer to the zealots, decreasing their confidence, the width of the stripe may change. Because of this additional step necessary to unblock the zealots, the spreading is slower than in the VM. Small domains last longer, and both the persistence and the number of interfaces are relatively larger.

The coalescence of domains, in one dimension, is driven by the diffusive behavior of the domain walls [37]. In order to better understand how the presence of zealots affects such behavior, we consider an initial state in which there is a single domain wall, located at $x(0)$, dividing the system into two blocks, each with one of the $\sigma_i = \pm 1$ states. The boundary conditions are open, $\gamma \to \infty$, and all sites start with $\eta_i = 0$. The mean square displacement $R^2(t) = [x(t) - x(0)]^2$, where $x(t)$ is the location of the interface at time t, is shown in Fig. 3 for different values of $\Delta\eta$. In all cases, two timescales are present. The initial behavior is purely diffusive, as in the VM (thin black line), and $R^2(t) \sim t$. The smaller $\Delta\eta$ is, the longer it will take for the system to deviate from the original VM behavior, becoming subdiffusive. This deviation occurs at an intermediate time that behaves as $(\Delta\eta)^{-1}$ when zealots first appear. On a longer timescale, which also goes as $(\Delta\eta)^{-1}$, the diffusive behavior is resumed. At the late stage of the dynamics, all activity is confined to the stripe between the two blocks of zealots, and the interface evolution depends on unblocking the neighboring zealots, which occurs on a longer timescale. The overall behavior is reminiscent of glassy systems, with a fast timescale associated with the Brownian motion inside the cage formed by neighboring particles and a slower timescale related to the slow restructuring of the cages themselves.

B. Two dimensions

In the extreme case $\gamma = 1$, as mentioned above, the confidence η_i never decreases, and the creation of zealots is irreversible. The self-induced disorder is thus quenched. If $\Delta\eta$

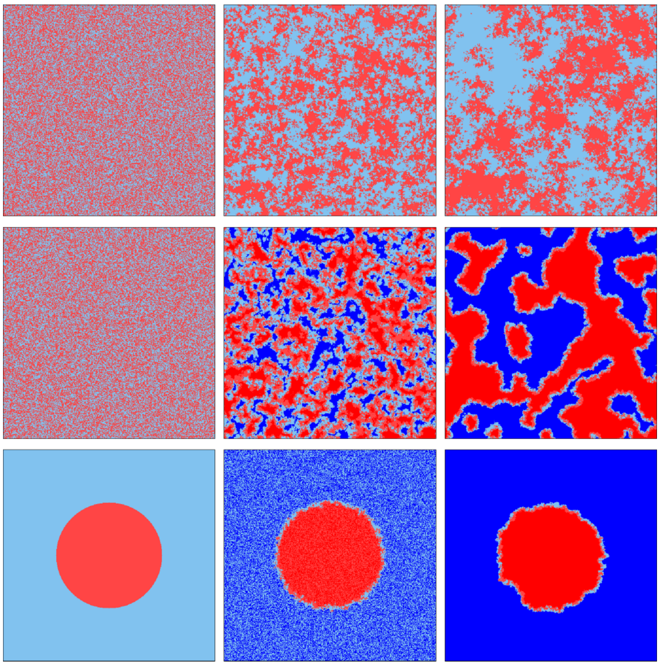

FIG. 4. Snapshots at different times for the 2D VM (top row) and our model (middle and bottom rows) with $\gamma \to \infty$ and $\Delta\eta = 10^{-2}$. Each color shows a different opinion, with the darker shades indicating zealots, while light colors represent normal agents. The onset of zealots induces an effective surface tension, and the bulk dynamics becomes curvature driven. Thus, while the interfaces between normal agents with opposite opinions (light red and light blue) are still rough as in the original VM, the internal walls between normal agents and zealots with the same opinion are smoother. Instead of a random initial state, in the bottom row we consider all agents with one opinion inside a circle, surrounded by the other opinion.

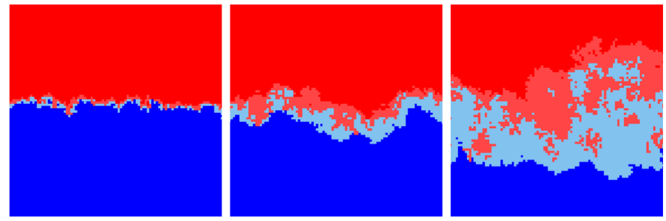

FIG. 5. Snapshots showing how the VM stripe develops, after 1000 MCSs, from a specially prepared initial state with two equal regions of opposite opinions in the $\gamma \to \infty$ case. Only the central part of the system is shown. From left to right the values of $\Delta\eta$ are, respectively, 1, 10^{-1}, and 10^{-2}. Notice that the active region gets wider as $\Delta\eta$ decreases with many small domains, without zealots, fully embedded in the opposite opinion.

is large enough, the compact domains of zealots grow very quickly until they collide with the neighboring domains. Thus, as in one dimension, the two-dimensional system with $\gamma = 1$ reaches a frozen state without normal agents, and consensus is avoided. We focus here, instead, on the $\gamma \to \infty$ case, where the confidence is fully reset after a single contact with a different opinion. For intermediate values of γ the system behavior interpolates between these two extremes. The results discussed below were averaged over at least 1000 samples.

The behavior of the case $\gamma \to \infty$ is illustrated in Fig. 4 when starting from a random initial state (middle row). For comparison, the evolution of the original VM is shown in the top row. Deep inside the domains, certainty builds up, and the agents become zealots, creating an internal interface between bulk zealots and normal agents. The presence of zealots induces an effective surface tension, and this interior interface gets smoother. The dynamics become curvature driven, similar to those of the out-of-equilibrium 2D Ising model, as shown in the snapshots in the middle and bottom rows of Fig. 4. As will be shown below, the analogy with the model A dynamical universality class [33], to which the out-of-equilibrium Ising model belongs, goes beyond these visual similarities. Being curvature driven, the circular domain shrinks [38–41], with a much reduced fragmentation when compared with a similar condition for the VM [10] (see also Fig. 10 below). Whatever the initial condition, the external interfaces remain rough at all times because normal agents with both opinions get confined in the VM superficial stripe. The fluctuations of the main interface cause a constant flipping that keeps the certainties below the threshold in this region, setting the average distance between the external and internal interfaces. The width of the VM stripe depends on both $\Delta\eta$ and γ, as illustrated in Fig. 5 for an initial state with a flat interface within two equal sized domains. For large values of $\Delta\eta$ zealots form very quickly, and the dynamics get blocked close to the initial state (notice that the initial state is absorbing for the IM0; left panel). As $\Delta\eta$ decreases, the VM stripe becomes wider, and both the roughness of the interface and the number of fragmented clusters increase (middle and right panels). Of course, when $\Delta\eta \to 0$, no zealot is formed, and the VM stripe is the whole system.

Figure 6 presents the behavior of the persistence $P(t)$. Similar to the 1D case, the initial regime is equivalent to the VM [9,45] because zealots are still absent. However, upon the sudden rise in the number of zealots (red solid line), $P(t)$ slows down and deviates from the VM curve (thin black line). For increasing system sizes, $P(t)$ develops a power-law

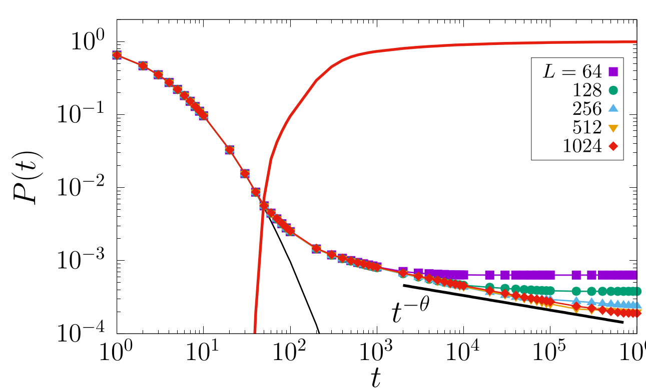

FIG. 6. Persistence $P(t)$ of increasing linear sizes L for $\Delta\eta = 10^{-2}$ and $\gamma \to \infty$. In the initial regime there are no zealots, and the behavior follows the VM ($L = 64$; thin black line). As the density of zealots increases (red thick line), $P(t)$ departs from this behavior and eventually develops a power law, $P(t) \sim t^{-\theta}$. The thick black line shows the 2D Ising behavior whose exponent, after a quench from high temperature, is $\theta \simeq 0.2$ [42–44].

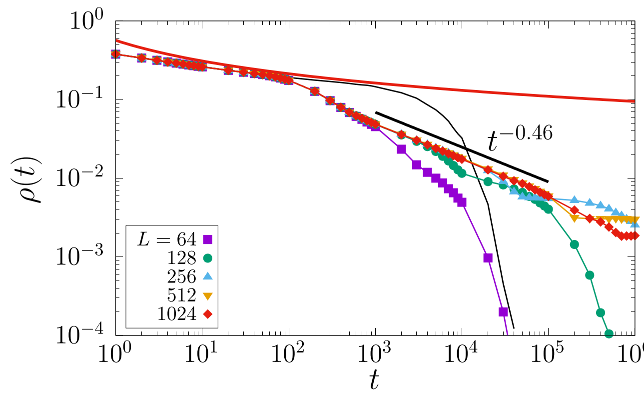

FIG. 7. Density of active interfaces $\rho(t)$, defined as the fraction of neighboring agents with different opinions, for $\Delta\eta = 10^{-2}$, $\gamma \to \infty$, and different sizes. The VM results for $L = 64$ are shown for comparison (thin black line) along with the expected, asymptotic behavior [8,11] (thick red line). Deviations from the VM behavior start again when zealots rapidly invade the lattice. Since domains become smoother, the total perimeter, measured by $\rho(t)$, presents a strong decrease relative to VM. For large enough systems, a power law with an exponent slightly below 1/2, $\rho(t) \sim t^{-0.46}$, develops.

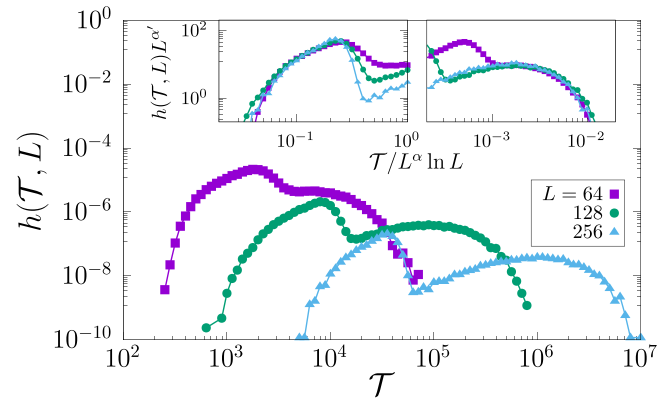

FIG. 8. Distribution $h(\mathcal{T}, L)$ of the consensus time $\mathcal{T}$ with $\Delta\eta = 10^{-2}$ and $\gamma \to \infty$. Our model, different from the VM, which has a single timescale [11], also develops a longer timescale related to transient stripes, similar to the IM0. Good collapses are obtained by rescaling the horizontal axis with $L^\alpha \ln L$: $\alpha \simeq 2$ for the first peak (left inset), and $\alpha \simeq 3.5$ for the second one (right inset). In the vertical direction, $\alpha' = 3.5$ for both peaks.

behavior (thick black line), $P(t) \sim t^{-\theta}$, whose exponent is consistent with the one for the 2D Ising model after a temperature quench from high temperature, $\theta \simeq 0.2$ [42–44]. Most of the persistent spins are in the zealot bulk region, and the fluctuating interface between different opinions must collide with the internal interface in order to destabilize the zealots, originating the slowdown.

Figure 7 shows the fraction $\rho(t)$ of links connecting neighboring agents with different opinions, i.e., located on the rough active interface that separates two domains. For $\gamma \to \infty$, sites belonging to a stripe whose width corresponds to the mean height of the surface will have a high probability of having small values of η_i, thus following the VM dynamics. After zealots are formed, $\rho(t)$ presents a strong decrease, deviating from the slow inverse logarithm behavior of the VM [8]. Moreover, for large enough systems, a power-law develops, $\rho(t) \sim t^{-0.46}$, whose exponent is consistent with the model A universality class, although it is slightly below 1/2. This deviation from the characteristic 1/2 exponent of the curvature-driven coarsening was observed in similar models [20,26,27,32]. Notice that although larger clusters have an underlying structural frame provided by the zealot bulk, smaller domains that are formed by fragmentation close to the surface are, in general, purely VM and contribute with a slower, logarithmic time dependence. This effect, along with those samples that have a longer lived metastable structure (see below), seems to be the main mechanism explaining this small exponent difference. Despite its short-range roughness that is analogous to the VM, the smaller value of $\rho(t)$ shown in Fig. 7 indicates that on a larger scale the clusters are more compact. This is a consequence of the bulk of sufficiently large domains, formed by zealots, whose growth is driven by curvature. The presence of these more compact regions has a strong influence on the long range properties of the VM region around the bulk, providing a rather smooth support that decreases the overall perimeter.

In the IM0, the asymptotic state is either fully magnetized or divided into multiple (most often two) parallel stripes [46–52], and either of these possible fates is decided early in the dynamics, when it approaches the percolative critical point [53–57]. The time to attain the former grows as $\mathcal{T} \sim L^2$ for most of the initial states [47]. However, a small fraction of these initial states develops diagonal stripes that slow down the dynamics, with the characteristic time increasing as $\mathcal{T} \sim L^{3.5}$ [47,48,52]. For the VM, since it lacks surface tension and straight interfaces are unstable, no structures resembling stripes are formed. All initial states do converge to consensus in a time whose average scales as $\langle\mathcal{T}\rangle \sim L^2 \ln L$ [6,7,11]. As a consequence, the single-peaked consensus time distribution $h(\mathcal{T}, L)$ obeys the scaling relation $h(\mathcal{T}, L) = L^{-\alpha'} H(\mathcal{T}/L^\alpha \ln L)$ [11]. In our model, once zealots are formed and curvature-driven dynamics becomes important, some initial states, with clusters that wrap the system in a single direction, develop transient structures that are similar to stripes. Nonetheless, since the dynamics at the surface are driven by interfacial noise, these stripes remain unstable, and the system eventually converges to consensus. Nonetheless, the presence of such stripes introduces a new timescale to attain consensus. This is the origin of the second peak in Fig. 8 for the distribution $h(\mathcal{T}, L)$ and has been observed in similar models [22,26–28,32]. The main contribution, however, comes from those initial states that are not delayed, and consensus is attained faster because, early in the dynamics, a percolating cluster, wrapping the system in two directions [11], forms. Notice that although a double-peak structure was also observed for the IM0 [52], in our model the second peak also has a contribution from those states whose stripes are parallel to the lattice directions, while in the IM0 they lead to absorbing states and only diagonally striped configurations contribute. In the left inset in Fig. 8 an excellent collapse is obtained with $L^\alpha \ln L$ and $\alpha \simeq 2$. This is similar to the L^2 scaling of the corresponding first peak for the IM0 but also includes the logarithmic correction from the VM [11]. The

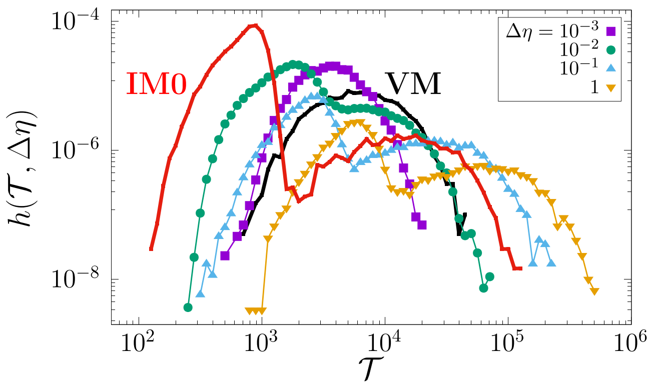

FIG. 9. Consensus time distribution $h(\mathcal{T}, L)$ for a single size, $L = 64$, and different values of $\Delta\eta$. For comparison, the VM (black line) and the IM0 (red line) are also shown. Averages over 10^4 samples were considered.

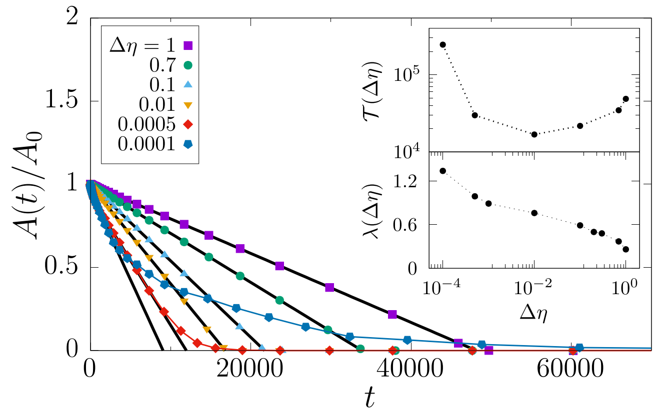

FIG. 10. Time evolution of the average area $A(t)/A_0$ of an initially circular domain containing a single opinion (Fig. 4, bottom row) for $L = 256$ and several values of $\Delta\eta$. Averages are over 1000 samples. The straight black lines are linear fits at short times, whose declivity λ is the rate at which the area shrinks (bottom inset). Notice that above the minimum for $\Delta\eta \gtrsim \Delta\eta_{\min} \approx 10^{-2}$, the linear behavior, characteristic of the Ising model [58,59], persists in the whole interval, while for smaller values, it crosses over to the logarithmic behavior. The average consensus time $\mathcal{T}(\Delta\eta)$ is shown in the top inset.

second peak collapse, with $\alpha \simeq 3.5$, is shown in the right inset.

Although one could expect a simple interpolation, by varying $\Delta\eta$ from the VM (when $\Delta\eta \to 0$) and the IM0 (for $\Delta\eta \to 1$), Fig. 9 shows that the dependence on $\Delta\eta$ is nontrivial. For $\Delta\eta = 10^{-3}$, there is a single, large peak in $h(\mathcal{T}, L)$. By slightly increasing $\Delta\eta$, a second peak appears, while the first one moves towards the position of the corresponding first peak of the IM0. After the location of this peak has attained its minimum value, this tendency is reversed for intermediate values of $\Delta\eta$ and starts approaching the position of the VM peak. Notice that, for all values of $\Delta\eta$, the first peak is within the first peak of the IM0 and the VM single peak. For $\Delta\eta = 1$, however, the whole distribution has the largest displacement away from the IM0 distribution. Thus, the active region on the surface of all clusters, whatever its width, always has a delaying effect. The second, smaller peak, once it forms, does not seem to present a minimum and always moves to larger times, becoming even larger (and wider) than the corresponding peak of the IM0.

In order to understand the origin of the above minimum, we consider a specially prepared initial state that prevents the formation of stripes. As illustrated in the bottom row of Fig. 4, one opinion is initially fully embedded in a circular domain while the other one surrounds it [17,20,30]. Figure 10 shows the time evolution of the relative area of the selected opinion $A(t)/A(0)$, regardless of the fragmentation that may occur on the surface. For very small values of $\Delta\eta$, the possible presence of zealots late in the dynamics has little impact, and the behavior is logarithmic, following the VM. As $\Delta\eta$ increases, the frozen bulk forms along with the VM region closer to the surface whose width depends on $\Delta\eta$. While the drop and its fragments decrease in size, the VM region roughly retains its width, forcing the internal border with the bulk (zealots) to recede and disappear. During the time interval when zealots are present, the behavior is linear, similar to that of the IM0, $A(t) \simeq A_0(1 - \lambda t)$. The parameter λ is a monotonically decreasing function of $\Delta\eta$ (bottom inset in Fig. 10). As $\Delta\eta$ increases from 10^{-4} to 1, λ decreases from, roughly, 1.4 to 0.2, while for the IM0, $\lambda \simeq 2$ [41] and the drop disappears faster than in all cases considered here. An interesting consequence is that the faster the initial linear decrease is ($\Delta\eta \to 0$), the sooner the behavior of $A(t)$ deviates from it. Moreover, for small $\Delta\eta$, once $A(t)$ becomes logarithmic, the average consensus time increases. On the other hand, for $\Delta\eta \to 1$, the VM region is very small, and because most of the agents are zealots, the dynamics slow down, and λ is small. In this case, even if the deviations from the linear behavior cannot be seen in the linear scale of Fig. 10, the average consensus time is large once again. Thus, $\langle\mathcal{T}\rangle$ has a minimum [18,19,24] at an intermediate value, close to $\Delta\eta \simeq 10^{-2}$. Note that although the above behavior is rather clear for a single droplet, once a more general, random initial state is considered, the trend for the average area is not (not shown). The probable origin is the VM region that dresses each compact bulk. Because it is easily fragmented, there is a large contribution of small domains to the average from sizes that are much less frequent in the IM0.

IV. CONCLUSIONS

We introduced an opinion model whose agents have intermediate levels of confidence that may interfere in their process of changing opinion. When all agents have low confidence, in the beginning of the dynamics, the model is equivalent to the VM, where a single contact with a different opinion is enough for an agent to change its own. Opinion reinforcement builds up confidence, and above a certain threshold, the agent becomes a kinetically constrained zealot whose opinion is frozen. But regardless of the nature of the agents, the variables characterizing their confidence keep evolving as the agents interact with their neighborhood. We considered two limiting cases depending on the parameter γ, which rescales the confidence after an agent is confronted with a different opinion. For $\gamma = 1$, the zealot state is irreversible, while for $\gamma \to \infty$ the dynamics allows the zealot state to be reversed and coexistence with normal voters. Similar opinions segregate in spatial domains, and in their bulk, because of the positive reinforcement, zealots first appear once the confidence threshold ϕ is attained. Because the zealots are frozen, there is an increased probability of repeated contacts with their nonzealot neighbors, increasing their confidence as well. This mechanism of noise reduction smooths the internal interface between zealots and normal voters with the same opinion. This smoother internal surface induces an effective surface tension, acting as a structural frame that turns the dynamics from interfacial noise to curvature driven. As a consequence, several properties become analogous to those of the low temperature Ising model with a nonconserved order parameter (IM0) in the Allen-Cahn (model A) universality class [33]. Close to a domain border, continued interaction with the opposite opinion keeps the confidence of these agents low. Normal agents are thus confined to this region, close to the surface, and their number depends on $\Delta\eta$, i.e., on how fast the zealot bulk grows. Although the curvature-driven growth was already observed in other variations of the VM [17,20,22,26–32], our model allows us to tune the number of normal voters close to the surface through $\Delta\eta$. Interestingly, the internal surface induces a curvature-driven growth, but the actual surface is driven by the interface noise typical of the VM, becoming rougher and more fragmented than in other models.

The width of the normal voter region close to the surface, which depends on $\Delta\eta$ (see Fig. 5), determines how fast the domains shrink and, consequently, the exit time, i.e., how long it takes to attain consensus. While a large domain shrinks, the zealot bulk disappears first, and that cluster dynamics is no longer driven by the curvature of the interface. This late regime is dominated by the normal voters, and the dynamics becomes logarithmic. How important this final regime will be depends on the width of the stripe with normal voters around the bulk. When $\Delta\eta$ is large, it is thin, and most of the dynamics is dominated by the curvature-driven mechanism induced by the zealots. However, despite being curvature driven, the dynamics is still slower than in the IM0 because of the large number of zealots: since they are frozen, it is first necessary to turn them into normal agents. On the other hand, for small $\Delta\eta$, the stripe is thick, and once the bulk disappears, leaving only the normal voters, there is a crossover to a slower, logarithmic regime. It is the interplay between both mechanisms that explains the existence of a minimum consensus time as a function of $\Delta\eta$, directly related to the superficial normal voters.

There are some possible generalizations of the model that would be interesting to investigate. For example, individual heterogeneities [60] in the values of γ, $\{\gamma_i\}$, can be considered. If some of the agents have $\gamma_i \leqslant 1$, they may become permanent zealots. Another possible modification is to reintroduce the conservation of the magnetization, which is present in the pure VM but broken in our model, by a local conservation rule [61]. Such conserved order parameter dynamics are known to be in a different universality class from the nonconserved case [33,62], and their effect in the present model is worth investigating.

ACKNOWLEDGMENTS

Work partially supported by the Brazilian agencies Conselho Nacional de Desenvolvimento Científico e Tecnológico (CNPq) and CAPES.

[1] C. Castellano, S. Fortunato, and V. Loreto, Rev. Mod. Phys. **81**, 591 (2009).
[2] A. Baronchelli, R. Soc. Open Sci. **5**, 172189 (2018).
[3] S. Redner, C. R. Phys. **20**, 275 (2019).
[4] M. Lynas, B. Z. Houlton, and S. Perry, Environ. Res. Lett. **16**, 114005 (2021).
[5] P. Sturgis, I. Brunton-Smith, and J. Jackson, Nat. Hum. Behav. **5**, 1528 (2021).
[6] P. L. Krapivsky, Phys. Rev. A **45**, 1067 (1992).
[7] T. M. Liggett, *Stochastic Interacting Systems: Contact, Voter and Exclusion Processes* (Springer, Heidelberg, 1999).
[8] L. Frachebourg and P. L. Krapivsky, Phys. Rev. E **53**, R3009 (1996).
[9] E. Ben-Naim, L. Frachebourg, and P. L. Krapivsky, Phys. Rev. E **53**, 3078 (1996).
[10] I. Dornic, H. Chaté, J. Chave, and H. Hinrichsen, Phys. Rev. Lett. **87**, 045701 (2001).
[11] A. Tartaglia, L. F. Cugliandolo, and M. Picco, Phys. Rev. E **92**, 042109 (2015).
[12] M. Mobilia, Phys. Rev. Lett. **91**, 028701 (2003).
[13] M. Mobilia and I. T. Georgiev, Phys. Rev. E **71**, 046102 (2005).
[14] M. Mobilia, A. Petersen, and S. Redner, J. Stat. Mech. (2007) P08029.
[15] S. Galam and F. Jacobs, Phys. A (Amsterdam, Neth.) **381**, 366 (2007).
[16] F. Colaiori and C. Castellano, J. Stat. Mech. (2016) 033401.
[17] L. Dall'Asta and C. Castellano, Europhys. Lett. **77**, 60005 (2007).
[18] H.-U. Stark, C. J. Tessone, and F. Schweitzer, Phys. Rev. Lett. **101**, 018701 (2008).
[19] H.-U. Stark, C. J. Tessone, and F. Schweitzer, Adv. Complex Syst. **11**, 551 (2008).
[20] L. Dall'Asta and T. Galla, J. Phys. A **41**, 435003 (2008).
[21] R. Lambiotte, J. Saramäki, and V. D. Blondel, Phys. Rev. E **79**, 046107 (2009).
[22] D. Volovik and S. Redner, J. Stat. Mech. (2012) P04003.
[23] A. C. R. Martins and S. Galam, Phys. Rev. E **87**, 042807 (2013).
[24] Z. Wang, Y. Liu, L. Wang, Y. Zhang, and Z. Wang, Sci. Rep. **4**, 3597 (2014).
[25] C. Brugna and G. Toscani, Phys. Rev. E **92**, 052818 (2015).
[26] F. Velásquez-Rojas and F. Vazquez, J. Stat. Mech. (2018) 043403.
[27] X. Castelló, V. M. Eguíluz, and M. San Miguel, New J. Phys. **8**, 308 (2006).
[28] X. Castelló, A. Baronchelli, and V. Loreto, Eur. Phys. J. B **71**, 557 (2009).
[29] W. Zhang, C. C. Lim, G. Korniss, and B. K. Szymanski, Sci. Rep. **4**, 5568 (2014).
[30] C. Doyle, S. Sreenivasan, B. K. Szymanski, and G. Korniss, Phys. A (Amsterdam, Neth.) **443**, 316 (2016).

[31] P. Roy and P. Sen, Phys. Rev. E **95**, 020101(R) (2017).
[32] S. Mukherjee, S. Biswas, and P. Sen, Phys. Rev. E **102**, 012316 (2020).
[33] A. J. Bray, Adv. Phys. **43**, 357 (1994).
[34] A. J. Bray, S. N. Majumdar, and G. Schehr, Adv. Phys. **62**, 225 (2013).
[35] B. Derrida, J. Phys. A **28**, 1481 (1995).
[36] B. Derrida, V. Hakim, and V. Pasquier, Phys. Rev. Lett. **75**, 751 (1995).
[37] H. Hinrichsen, Adv. Phys. **49**, 815 (2000).
[38] H. C. Kang, W. H. Weinberg, and M. W. Deem, Phys. Rev. B **43**, 11438 (1991).
[39] A. Karma and A. E. Lobkovsky, Phys. Rev. E **71**, 036114 (2005).
[40] R. Cerf and S. Louhichi, Probab. Theory Relat. Fields **137**, 379 (2007).
[41] J. J. Arenzon, L. F. Cugliandolo, and M. Picco, Phys. Rev. E **91**, 032142 (2015).
[42] B. Derrida, A. J. Bray, and C. Godrèche, J. Phys. A **27**, L357 (1994).
[43] D. Stauffer, J. Phys. A **27**, 5029 (1994).
[44] T. Blanchard, L. F. Cugliandolo, and M. Picco, J. Stat. Mech. (2014) P12021.
[45] M. Howard and C. Godrèche, J. Phys. A **31**, L209 (1998).
[46] B. Derrida, P. M. C. de Oliveira, and D. Stauffer, Phys. A (Amsterdam, Neth.) **224**, 604 (1996).
[47] A. Lipowski, Phys. A (Amsterdam, Neth.) **268**, 6 (1999).
[48] V. Spirin, P. L. Krapivsky, and S. Redner, Phys. Rev. E **63**, 036118 (2001).
[49] V. Spirin, P. L. Krapivsky, and S. Redner, Phys. Rev. E **65**, 016119 (2001).
[50] K. Barros, P. L. Krapivsky, and S. Redner, Phys. Rev. E **80**, 040101(R) (2009).
[51] J. Olejarz, P. L. Krapivsky, and S. Redner, Phys. Rev. Lett. **109**, 195702 (2012).
[52] C. Godrèche and M. Pleimling, J. Stat. Mech. (2018) 043209.
[53] J. J. Arenzon, A. J. Bray, L. F. Cugliandolo, and A. Sicilia, Phys. Rev. Lett. **98**, 145701 (2007).
[54] A. Sicilia, J. J. Arenzon, A. J. Bray, and L. F. Cugliandolo, Phys. Rev. E **76**, 061116 (2007).
[55] T. Blanchard, F. Corberi, L. F. Cugliandolo, and M. Picco, Europhys. Lett. **106**, 66001 (2014).
[56] T. Blanchard, L. F. Cugliandolo, M. Picco, and A. Tartaglia, J. Stat. Mech. (2017) 113201.
[57] A. de Azevedo-Lopes, R. A. L. Almeida, P. M. C. de Oliveira, and J. J. Arenzon, arXiv:2206.05808.
[58] M. Grant and J. D. Gunton, Phys. Rev. B **28**, 5496 (1983).
[59] P. S. Sahni, G. S. Grest, and S. A. Safran, Phys. Rev. Lett. **50**, 60 (1983).
[60] N. Masuda, N. Gibert, and S. Redner, Phys. Rev. E **82**, 010103(R) (2010).
[61] F. Caccioli, L. Dall'Asta, T. Galla, and T. Rogers, Phys. Rev. E **87**, 052114 (2013).
[62] A. Sicilia, Y. Sarrazin, J. J. Arenzon, A. J. Bray, and L. F. Cugliandolo, Phys. Rev. E **80**, 031121 (2009).